Materials Science and Engineering A368 (2004) 88–93

www.elsevier.com/locate/msea

Mechanical properties and microstructure of aluminum alloy 2618 with $Al_3(Sc, Zr)$ phases

Kun Yu*, Wenxian Li, Songrui Li, Jun Zhao

College of Materials Science and Engineering, Central South University, Changsha Hunan 410083, PR China

Received 15 May 2003; received in revised form 25 September 2003; accepted 25 September 2003

Abstract

The tensile properties of a 2618 (Al–Cu–Mg–Fe–Ni) alloy containing scandium and zirconium were measured at 293, 473, 523 and 573 K to study the temperature influences on the experimental alloys. The microstructure was observed by using optical microscopy, scanning electron microscopy (SEM) and transmission electron microscopy (TEM). It was found that the addition of scandium and zirconium to 2618 alloy resulted in a primary $Al_3(Sc, Zr)$ phase. Such phase could refine the alloy grains because it acted as a core of heterogeneous crystallization during solidification. The secondary $Al_3(Sc, Zr)$ particles that precipitated from the α(Al) solid solution were fully coherent with the matrix and had an obvious precipitation hardening effect. They also made the S′ phase precipitate more homogeneously. The strengths of the 2618 alloy with $Al_3(Sc, Zr)$ phases increased at both ambient and elevated temperatures, without a decrease of ductility.

Keywords: AA2618; $Al_3(Sc, Zr)$ phase; Phase transformation

1. Introduction

It is difficult for ordinary aluminum alloys to provide enough strength, toughness and microstructure stability at elevated temperatures above 473 K. Although the alloys produced by rapid solidification (RS) processing, such as RS Al–Fe–V–Si series alloys, tend to have good mechanical properties up to 573 K, it is relatively more costly and more difficult to produce than the wrought alloys fabricated by the ingot metallurgy (IM) method [1,2]. Accordingly, an attempt in this research has been made to produce an IM wrought Aluminum alloy that maintains a high strength at elevated temperature (473–573 K). In recent years, several publications have been concerned with the addition of scandium to aluminum alloys to form a thermo-stable $L1_2$-type ($AuCu_3$) Al_3Sc phase and to obtain a significant strengthening improvement [3–5]. Yelagin and Zakharov [6] found that the addition of zirconium in Al–Sc system can contribute to form a ternary phase $Al_3(Sc, Zr)$ that has even better thermal stability and precipitation hardening effect than Al_3Sc phase does. However, the previous studies seldom report the influence of scandium and zirconium on the typical age-hardenable Al–Cu–Mg series alloys. Compared to other 2XXX series alloys, alloy 2618 (Al–Cu–Mg–Fe–Ni series) has good elevated temperature strength [7]. Therefore, in present investigation, trace scandium and zirconium were added to alloy 2618 to evaluate and discuss the influences of $Al_3(Sc, Zr)$ phase on its mechanical properties.

2. Experimental

The chemical composition (mass%) of the experimental alloy used is as follows: Al–2.23Cu–1.21Mg–0.93Fe–1.09Ni–0.30Sc–0.30Zr (Alloy A). Another alloy (Alloy B) was also prepared with the same composition as AA2618 for a comparison. The cast billets of experimental alloys were hot-rolled at 723 K and cold-rolled into sheets of 2 mm thickness. The reductions of final cold process were about 50 and 75%, respectively. After cold rolling, some plate specimens were annealed at different temperatures ranging from 423 to 773K for 1 h. Others were solution treated in a salt bath at 783–788 K for 30 min and water quenched. Then, they were

* Corresponding author. Tel.: +86-731-8830261; fax: +86-731-8876692.
E-mail address: kunyu2001@sina.com (K. Yu).

0921-5093/$ – see front matter © 2003 Elsevier B.V. All rights reserved.
doi:10.1016/j.msea.2003.09.092

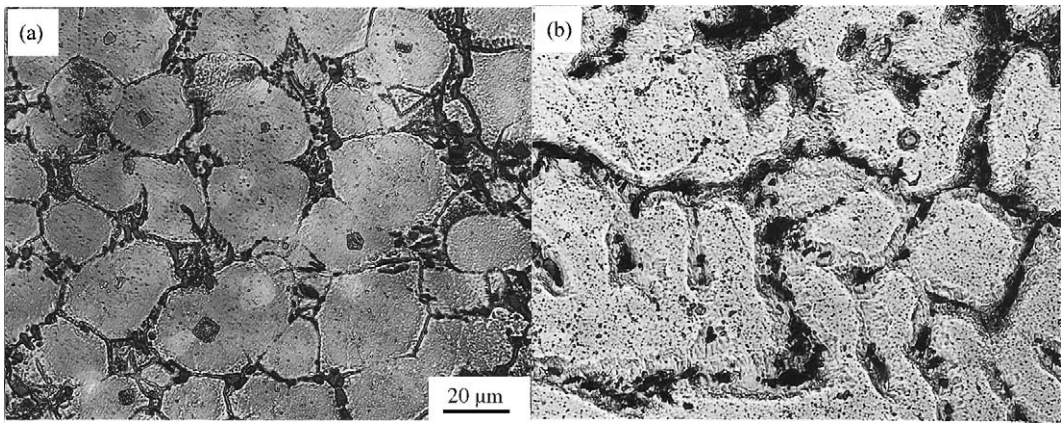

Fig. 1. Morphology of Alloys A and B in the as-cast state: (a) as-cast Alloy A and (b) as-cast Alloy B.

immediately aged at 473 and 573 K, respectively. The hardness measurements of both the annealed and aged specimens were made at room temperature by using HVA-10A Vickers hardness tester with a load 9.8N. The tensile test specimens that aged at 473 K for about 18–0 h were held at the elevated temperatures for 15 min, then performed on an INSTRON 8032 mechanical testing machine. Microstructures of the alloy were observed by using Nephoto-2 optical microscope, H-800 transmission electron microscope and KYKY-1000B scanning electron microscope.

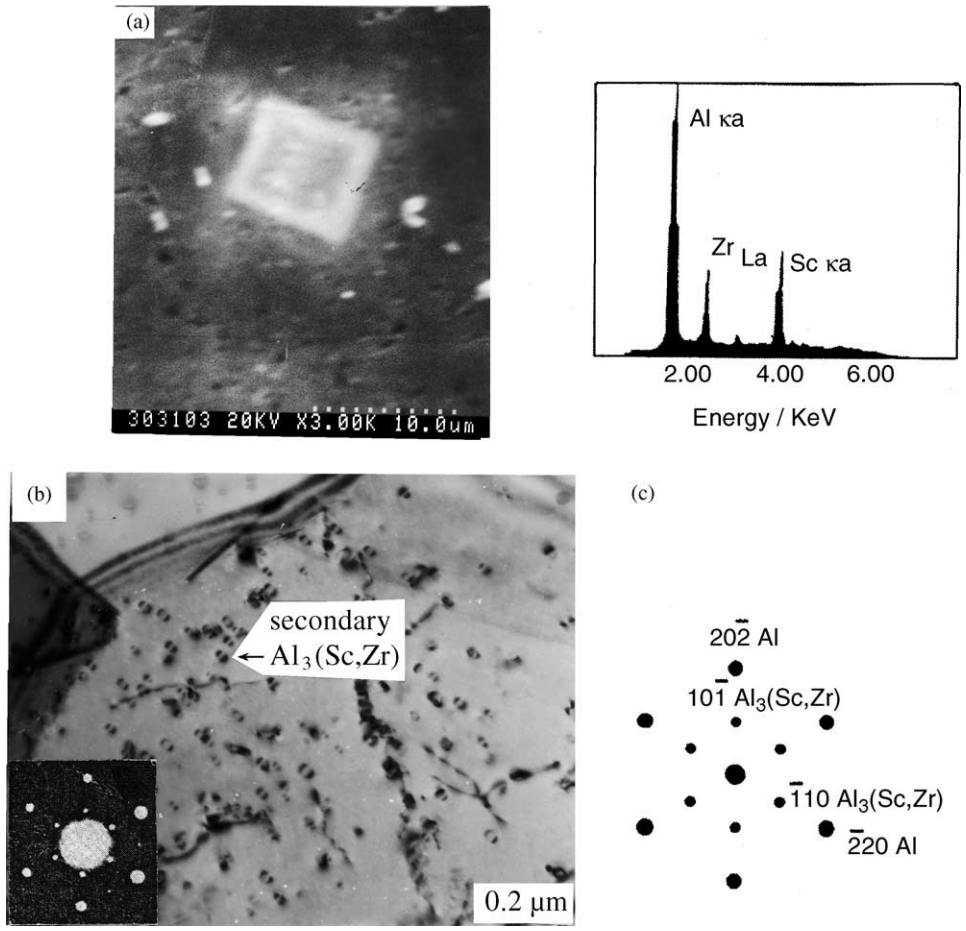

Fig. 2. Morphologies and composition of phases $A1_3$(Sc, Zr) in the as-cast state: (a) the cubic morphology of primary phase $A1_3$(Sc, Zr); (b) the composition of phase $A1_3$(Sc, Zr) and (c) the secondary Al_3(Sc, Zr) particles in Alloy A.

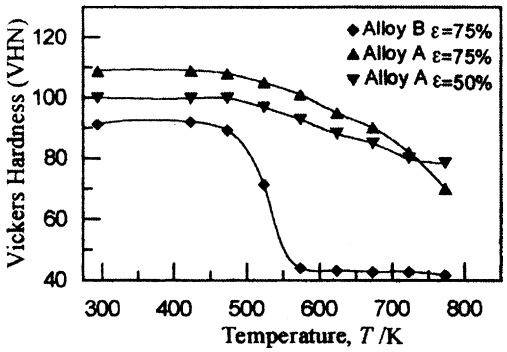

Fig. 3. Hardness variation of Alloys A and B during annealing temperatures.

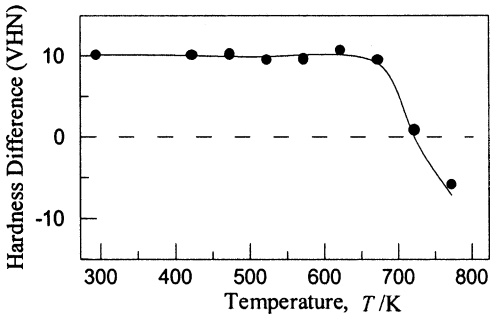

Fig. 4. ΔH-temperature curves of Alloy A.

3. Results and discussion

3.1. Microstructure of alloys in the as-cast state

The morphologies of alloys A and B in the as-cast states are shown in Fig. 1. The grain size of Alloy A (about 20–30 μm) is smaller than that of Alloy B (about 100 μm). There is a phase with a cubic morphology in the center of the grain of Alloy A (Fig. 1(a)). The back-scattered scanning electron micrograph and the composition analysis of such phase shows that it contains aluminum, scandium and zirconium atoms (Fig. 2(a)). Based upon the Al–Sc–Zr phase diagram [8], it is a primary Al_3Sc/Al_3Zr compound because the composition of scandium is less than 0.4%, zirconium is less than 0.4%, and the scandium to zirconium ratio is greater than 0.5.

The TEM micrograph of Alloy A in the as-cast condition (Fig. 2(b)) shows that the secondary $Al_3(Sc, Zr)$ particles

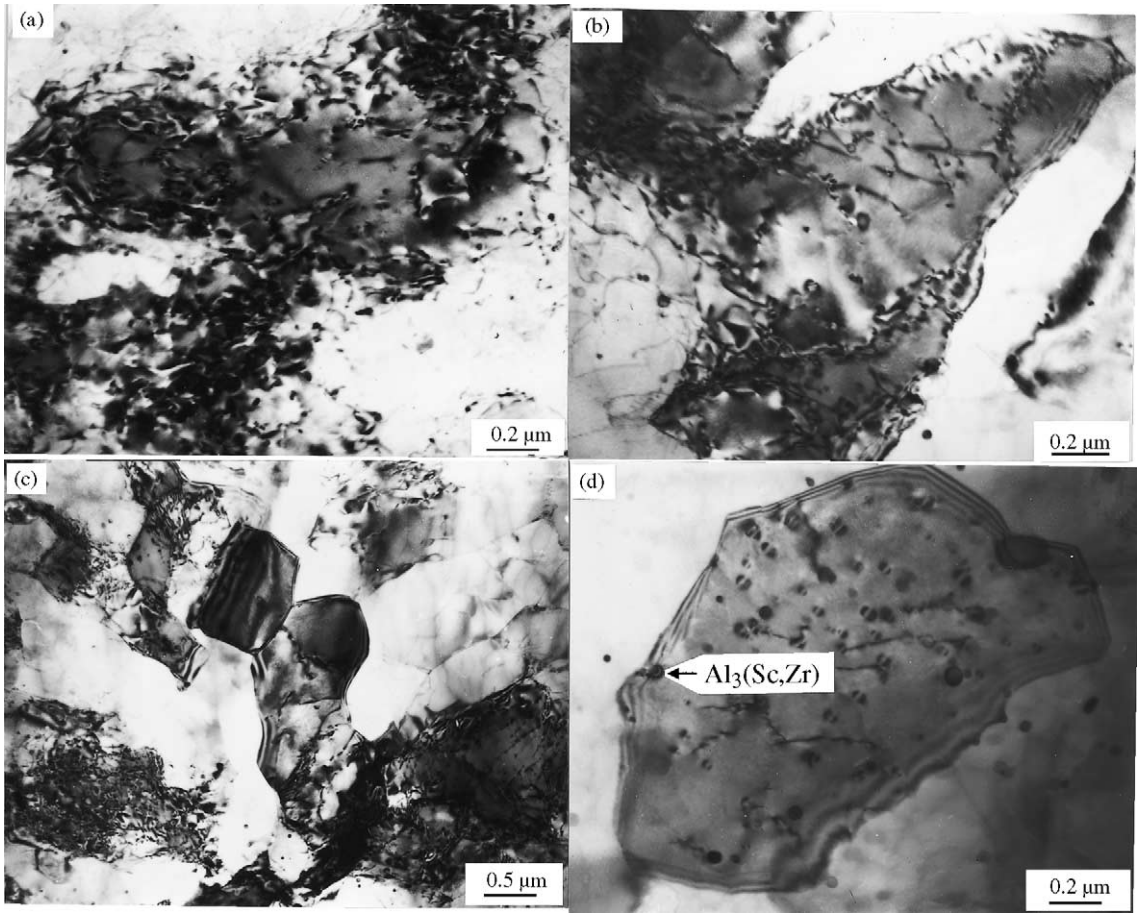

Fig. 5. Microstructures of Alloy A on different annealing temperatures for 1 h: (a) at cold-rolled state; (b) annealed at 573 K; (c) annealed at 673 K and (d) annealed at 773 K.

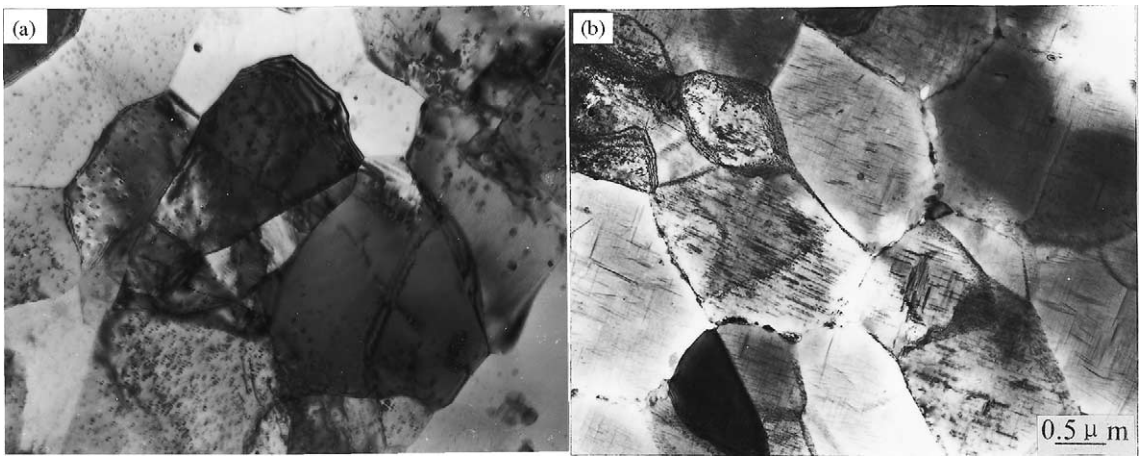

Fig. 6. Microstructures of Alloy A: (a) in the as-quenched state and (b) aged on 473 K on 20 h.

(with double-arc contrast) precipitate from the solid solution of matrix. The [1 1 1] orientation diffraction pattern from $Al_3(Sc, Zr)$ particles shows a super lattice spots due to the ordered nature of the $L1_2$ structure.

In the Al_3Sc/Al_3Zr compound, zirconium atoms substitute some of the scandium atoms in the Al_3Sc unit cell, and its chemical formula might be more accurately written as $Al_3Sc–Al_3Sc_{1-x}Zr_x$ [8–10], where x is a variable that depends on the content of zirconium in the alloy. The $Al_3(Sc, Zr)$ phase has a structure of $L1_2$ type and is characterized by a structural and dimensional matching with the aluminum matrix. Therefore, the primary $Al_3(Sc, Zr)$ phase forms in the center of alloy grains, acts as the nuclei of heterogeneous crystallization in the melt and leads to the grain refinement of the experimental alloy. The mechanism of aluminum grows from the particles was discussed in reference [8,11].

3.2. Hardness variation and microstructure during annealing treatment

The hardness variations of Alloys A and B at different temperatures are shown in Fig. 3. It is worth noting that the hardness of Alloy B decreases significantly in the temperature range from 473 to 573 K due to the recrystallization during the annealing. But under the same condition, the recrystallization phenomenon in Alloy A is not clearly identified due to a slow decreasing of hardness.

In order to obtain the recrystallization temperature of Alloy A, the hardness difference of Alloy A under different deformations was measured as a function $\Delta HV = HV\varepsilon_1 - HV\varepsilon_2$ (where $\varepsilon_1 = 75\%$, $\varepsilon_2 = 50\%$). The results are shown in Fig. 4. The temperature range in which the value of ΔHV decreased greatly may be treated as the beginning of primary recrystallization [12].

The morphology of Alloy A after different annealing temperatures are shown in Fig. 5. In the cold-rolled state, many dislocations exist in the matrix. During the process of annealing, the dislocations become fewer and the recrystallization sub-grains and grains form.

The second phases in the alloy will influence the process of recrystallization [8,13]. In the alloy AA2618, the typical hard particles Al_9FeNi act as preferential sites for increasing the dislocation density during cold work because the particles produce a turbulent and complex deformation pattern around themselves. As a result, the particles provide preferential sites for the nucleation of recrystallization during annealing because of the increased strain energy in the matrix around these particles.

But the $Al_3(Sc, Zr)$ phase can impede the process of recrystallization. The force applied by $Al_3(Sc, Zr)$ particles to retard the recrystallization can be expressed as [13]:

$$P_Z = \frac{3f\gamma}{2r} \quad (1)$$

where γ is the boundary energy between the phase and matrix, f the volume fraction of $Al_3(Sc, Zr)$ particles, and r the average size of the dispersoid (about 20–30 nm for $Al_3(Sc, Zr)$ particles). As the value of f/r is large due to the very small size of $Al_3(Sc, Zr)$ particles, the impeding force is great and the speed of recrystallization is slowed.

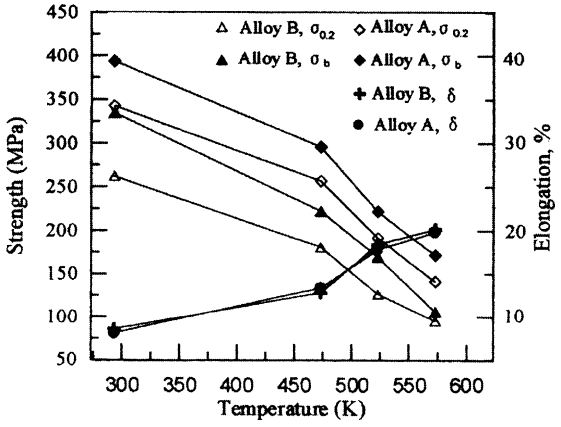

Fig. 7. Tensile properties of alloys at different temperatures.

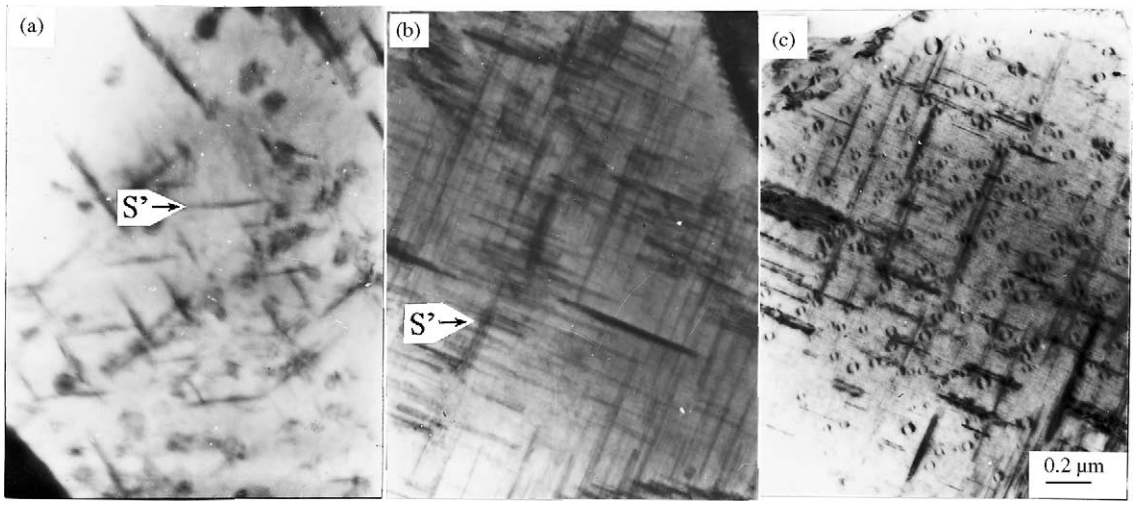

Fig. 8. Morphology of S′ and Al_3(Sc, Zr) phase in Alloy A. (a) S′ phase in Alloy (B) $A1_3$(Sc, Zr) phase in Alloy A (c) S′ + $A1_3$(Sc, Zr) phase in Alloy A.

Furthermore, Al_3(Sc, Zr) particles have extreme thermal stability. With the temperature increasing, the Al_3(Sc, Zr) particles obtain a low coarsening rate [14]. This can be shown in Fig. 8 that the Al_3(Sc, Zr) particles are only 30–40 nm in diameter after being aged at 723–773 K. Therefore, the recrystallization of Alloy A is retarded by the thermo-stable phase Al_3(Sc, Zr) through their impeding the nucleation and growth process of recrystallized grains.

3.3. Mechanical properties and microstructure during aging treatment

The tensile properties of Alloy A at 293, 473, 523 and 573 K are shown in Fig. 6 where they may be compared with the values of Alloy B. It should be noted that the ambient and elevated temperature strengths of Alloy A were obviously greater than those of Alloy B. The yield strength and ultimate strength of Alloy A increases by about 80 MPa at ambient temperature and 40 MPa at 573 K with almost no ductility changes.

The increment of alloy strength can be treated as the effects of Al_3(Sc, Zr) particles. First, the micrographs of Alloy A in as-quenched and peak-aged states show that there are many double-layer Al_3(Sc, Zr) phase (Fig. 7). This means it is full coherent with the matrix [15]. The Al_3(Sc, Zr) particles and the aluminum-matrix must be strained by equal opposite force because of the particle's coherence. A high coherent strain energy exists in the matrix around the Al_3(Sc, Zr) particles and produces a coherent strengthening.

Second, the size of the precipitates of Al_3(Sc, Zr) is about 20–30 nm and the Orowan strength mechanism operates. So the small and dispersed Al_3(Sc, Zr) particles will provide a large force to retard the movement of dislocations and increase the alloy strength.

Third, the Al_3(Sc, Zr) particles allow the needle shape phase S′, a dominated strengthening phase in Al–Cu–Mg alloy, to precipitate more homogeneously and dispersedly (Fig. 8). The normal sequence of S phase precipitates in Al–Cu–Mg alloy is: super-saturated solid solution (SSS) → Guinier–Preston–Bogaryatskii (GPB) zone → (metastable phase) → S [16]. Because the coherent strain field of Al_3(Sc, Zr) particles produced in the matrix, they provide favorable places for S′ phase to form. And the Al_3(Sc, Zr) particles can stabilize the sub-grain boundaries and dislocations that are also the preferential nucleation sites for S′ phase. The more dispersed S′ phase is, the higher the alloy strength is. Fig. 8 shows the S′ phase in Alloy A is thinner and more dispersed than that of Alloy B. And both the S′ and Al_3(Sc, Zr) phases can act as the strengthen phases.

4. Conclusions

(1) The primary Al_3(Sc, Zr) phase, as a core, plays a important role during the process of heterogeneous crystallization, so the grains of the experimental alloy containing scandium and zirconium are refined.
(2) The recrystallization temperature of the experimental alloy containing scandium and zirconium is about 200 K higher than that of AA2618. The thermo-stable Al_3(Sc, Zr) particles can impede the nucleation of recrystallization grains and retard their growth.
(3) The secondary Al_3(Sc, Zr) phase is fine coherent with the matrix. It has coherent strengthening and precipitation hardening effects. It also makes the S′ phase precipitate more homogeneously. So the tensile strengths of alloy increase both at ambient and elevated temperatures.

References

[1] S.M. Kazanjian, N. Wang, Mater. Sci. Eng. A 234–236 (1997) 571.
[2] Z. Wang, R. Tian, in: Manufacture Handbook of Al Alloy, Central South University of Technology Press, Changsha, 1989, p. 75.

[3] N. Blake, M.A. Hopkins, J. Mater. Sci. 20 (1985) 2861.
[4] R.R. Sawtell, C.L. Jensen, Metall. Trans. 21A (1990) 421.
[5] L.S. Toropova, D.G. Eskin, M.L. Kharakterova, Advanced Aluminium Alloys Containing Scandium, Gordon and Breech, The Netherlands, 1998.
[6] V.I. Yelagin, V.V. Zakharov, Phys. Met. Metall. 60 (1985) 88.
[7] S.C. Bergsma, X. Li, J. Mater. Eng. Perform. 5 (1996) 100.
[8] L.S. Toropova, Phys. Met. Metall. 70 (1990) 106.
[9] A.F. Norman, R.S. Mcewen, P.B. Prangnell, Acta Mater. 46 (1998) 5715.
[10] K.B. Hyde, A.F. Norman, P.B. Prangnell, Acta Mater. 49 (2001) 1327.
[11] C.B. Fuller, A.R. Kranse, D.C. Dunand, Mater. Sci. Eng. A 338 (2002) 8.
[12] S. Gerelik, in: Recrystallization in Metals and Alloys, MIR Publishers, Moscow, 1981, p. 299.
[13] W.M. Mao, in: Recrystallization and Grain Growth of metals, Metallurgy Industry Press, Beijing, 1994, p. 77.
[14] K. Yu, S. Li, W. Li, J. Mater. Sci. Tech. 16 (2000) 416.
[15] L.I. Kaygorodova, V.P. Domashnikov, Phys. Met. Metall. 68 (1989) 160.
[16] D.A. Porter, K. Esteling, in: Phase Transformations in Metals and Alloys, Alden Press, Oxford, 1981, p. 24.